

Flat'n'Fold: A Diverse Multi-Modal Dataset for Garment Perception and Manipulation

Lipeng Zhuang¹, Shiyu Fan¹, Yingdong Ru¹, Florent Audonnet¹,
Paul Henderson¹ and Gerardo Aragon-Camarasa¹

Abstract— We present Flat'n'Fold, a novel large-scale dataset for garment manipulation that addresses critical gaps in existing datasets. Comprising 1,212 human and 887 robot demonstrations of flattening and folding 44 unique garments across 8 categories, Flat'n'Fold surpasses prior datasets in size, scope, and diversity. Our dataset uniquely captures the entire manipulation process from crumpled to folded states, providing synchronized multi-view RGB-D images, point clouds, and action data, including hand or gripper positions and rotations. We quantify the dataset's diversity and complexity compared to existing benchmarks and show that our dataset features natural and diverse manipulations of real-world demonstrations of human and robot demonstrations in terms of visual and action information. To showcase Flat'n'Fold's utility, we establish new benchmarks for grasping point prediction and subtask decomposition. Our evaluation of state-of-the-art models on these tasks reveals significant room for improvement. This underscores Flat'n'Fold's potential to drive advances in robotic perception and manipulation of deformable objects. Our dataset can be downloaded at <https://cvas-ug.github.io/flat-n-fold>

I. INTRODUCTION

Manipulating garments remains a significant challenge in robotics. Tasks such as flattening and folding require understanding the vast space of configurations that garments can adopt [1], [2], and planning complex sequences of actions accordingly [3], [4]. This makes it vital to have large, diverse datasets from which to learn effective perception models and manipulation strategies. However, current efforts to capture a representative dataset of garments being manipulated [2], [5], [6] are limited in their utility for developing advanced robotic capabilities, due to their relatively small scope and diversity, as well as a lack of ground-truth action annotations.

In this paper, we introduce a novel dataset, *Flat'n'Fold* (Fig. 1), which includes 1,212 human and 887 robot demonstration sequences across 44 unique garments within eight categories and surpasses existing datasets in size, scope, and diversity (Tab. I). Flat'n'Fold is a multi-view, multi-modal dataset that captures the process of flattening and folding different garments, starting from a crumpled garment. Specifically, our dataset includes:

- Human Demonstrations, where twenty human participants performed the flattening and folding tasks. Our objective is to capture a wide array of human strategies in garment handling and the diversity and complexity of garment manipulation tasks.

¹ School of Computing Science, University of Glasgow, G12 8QQ, Scotland, United Kingdom Lipeng.Zhuang@glasgow.ac.uk; gerardo.aragoncamarasa@glasgow.ac.uk

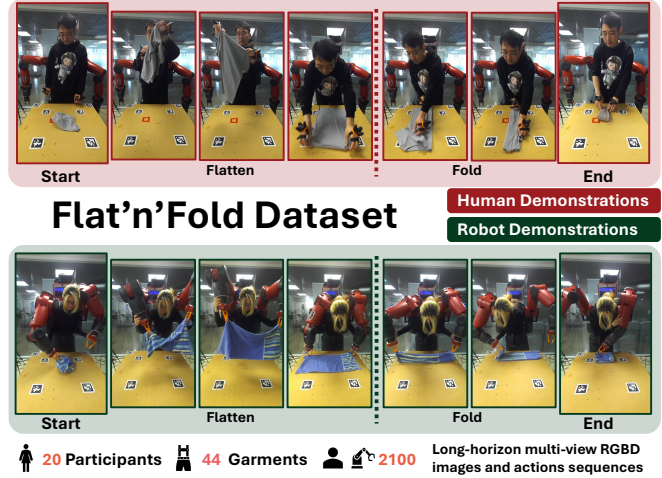


Fig. 1. Human and robot demonstrations: Each demonstrates the progression from a crumpled garment configuration to a flattened and folded state.

- Human-controlled Robot Demonstrations, where an expert human operator controls a robot to execute similar garment manipulation tasks, aiming to replicate natural, human-like approaches within the robot's operational limitations.

Moreover, our dataset is the first to include synchronized RGB-D image sequences with the position and rotation of the participants' hands (in human demonstrations) and robot grippers (in robot demonstrations), as well as camera parameters. To show the utility of our dataset, we set new benchmarks and baseline metrics for:

- *Grasping point detection* with 6,329 annotated point clouds from the human demonstrations and 5,574 from the robot demonstrations dataset. For this, we evaluated two popular models, PointNet++ and Point-BERT, and established a performance baseline.
- *Subtask decomposition from human and robot demonstrations* with $\sim 20,000$ annotated sub-task boundaries corresponding to 'pick' and 'place' actions.

II. RELATED WORK

Human demonstrations significantly enhance robotic training by providing detailed examples of natural, dexterous manipulations from which to learn (e.g. [4], [11]–[13]), instead of defining inflexible manipulation strategies by hand [1], [3], [14], [15]. Human demonstrations have shown to be essential for long-horizon tasks for manipulating rigid and

TABLE I
COMPARATIVE ANALYSIS WITH OTHER DATASETS, * INDICATES THAT THE SUBSET RELATED TO DEFORMABLE OBJECTS (OR GARMENTS) IS CONSIDERED.

Dataset	Agent	Setting	Garment Cat.	#Garments	#Seq.	#Frame	Deform.	Task	Vis. Info	Hum. Action	Ann.	Total Hrs.
VideoFolding [2]	Human	Real	3	-	1000	304k	Large	Flattening & Folding	Multi-view RGBD	x	Arm keypoint	8.5h
DeepDeform [5]	Human	Real	1	~110	400	39k	Medium	Move	Single-view RGBD	x	Sparse keypoint	-
Garment Tracking [7]	Human	Virtual	4	-	-	790k	Large	Flatten&Folding	Rendered Multi-view RGBD	-	Garment & Hand pose	-
VR [8]	Human	Virtual	3	3	60	-	Medium	Folding	Virtual Reality	-	-	-
Semantic State Est. [6]	Human	Real	1	18	-	33.6K	Medium	Pick-up & Folding	RGB	x	Cloth semantic state	-
Roboturk* [9]	Robot	Real	3	3	920	-	Medium	Flatten	Multi-view RGBD	-	-	~33h
MIME* [10]	Human&Robot	Real	1	~5	~265	-	Small	Wipe(no manipulation)	Single-view RGBD	x	-	-
Flat'n'Fold (ours)	Human&Robot	Real	8	44	2112	~1600k	Large	Flattening & Folding	Multi-view RGBD & Pointcloud	✓	Grasping point&time	>100h

simple deformable objects [16] and have enabled robots to anticipate future states and make decisions by optimizing policies throughout the task’s duration [17], [18].

Several existing datasets of human demonstrations of manipulating deformable objects have been used to train robotic systems for various tasks. However, these datasets are limited and have not let robots acquire all the skills necessary to manipulate garments, as shown in Fig. 1. For example, the MIME dataset [10] provided video demonstrations of 20 tasks but focused on rigid objects. That is, only one task involved a deformable object, *wiping with a cloth*, which was captured using single-view RGB-D data. DeepFashion [19] included only clothing and was intended for recognition tasks such as classification and attribute recognition rather than manipulation. Similarly, DeepDeform [5] presented an approach for non-rigid reconstruction of dynamic objects using RGB-D cameras. Tzelepis *et al.* [6] introduced a dataset of RGB images of human demonstrations while handling a tablecloth with the aim of semantic state estimation. However, the tasks considered were relatively simple (e.g. lifting and diagonal fold) and lacked complex manipulation sequences. The Video Human Demonstration dataset [2] consisted of Kinect cameras mounted on a folding table, and 1,000 folding demonstrations were captured from multiple angles and participants. While this dataset provides RGB-D images and skeleton keypoints of human actions, it did not include 3D spatial position and rotation information (nor camera parameters that could be used to infer these), which are required for imitation learning and policy learning in robotics.

Similarly, existing datasets relevant to deformable objects that use robot demonstrations or surrogate systems remain limited in scope and diversity. For instance, GarmentTracking [7] introduced the VR-Garment recording system, which enabled users to interact with virtual garment models via a VR interface. The VR-Folding dataset was introduced and included complex garment poses for tasks such as flattening and folding. However, the VR-Folding dataset was inherently bound to virtual reality (VR) environments, which introduced limitations in terms of its relevance to practical robotic operations in real-world scenarios. For real-world applications, Boix-Granell *et al.* [8] designed a Unity-based 3D platform using an HTC Vive Pro system for tablecloth manipulations only. Similarly, Moletta *et al.* [15] attempted to automate cloth folding with a system that

employed skeleton representations to generate folding plans. Although this helped replicate specific folding techniques, only three garment classes and fixed folding procedures were considered, reducing its adaptability to the diverse techniques required in real-world settings. Another significant work, the Roboturk dataset [9], used a smartphone-based 6-DoF controller with cloud integration, and a robotic arm was used to smooth out garments such as hand towels, jeans, or t-shirts on a table. Roboturk captured these sequences from a single camera perspective, restricting its application for complex tasks that require dual-arm coordination or depth perception.

To overcome the limitations of existing datasets, we introduce Flat’n’Fold, a dataset comprising human and robot demonstrations, including various garment types, manipulation tasks, and garment flattening and folding sequences, providing visual and action information. Tab. I compares our Flat’n’Fold dataset against existing datasets focused on human demonstrations and robotic manipulation of garments. In the table, ‘Agent’ represents whether it is human demonstrations or robot demonstrations; ‘Hum. Action’ means whether human action data is recorded and saved during human demonstrations; ‘Ann.’ represents extra annotations. Flat’n’Fold has a clear advantage in terms of data volume, diversity, and modalities recorded.

III. MATERIALS AND METHODOLOGY

A. Hardware

The hardware used is shown in Fig. 2. The setup for the human demonstration dataset integrates visual and motion information from three ZED2i cameras, a VR controller, and three mechanical pedals interfaced via USB. The ZED2i cameras were positioned to provide multiple views and minimize occlusions from human arms during garment manipulation. These views encompass the front, top, and back of the garment. The ZED2i cameras recorded 1080p images at 15Hz. For motion tracking, we used SteamVR [22] with two HTC Vive Trackers, where the VR headset [20] served as the world coordinate frame to which robot and tracker reference frames are linked. Two HTC Vive Trackers were affixed to the backs of participants’ hands, capturing position and rotation in 3D space relative to the headset at 15Hz. Three pedals were used to record the timing of actions involving the left or right hands and both hands, annotating when participants grasped or released the garment.

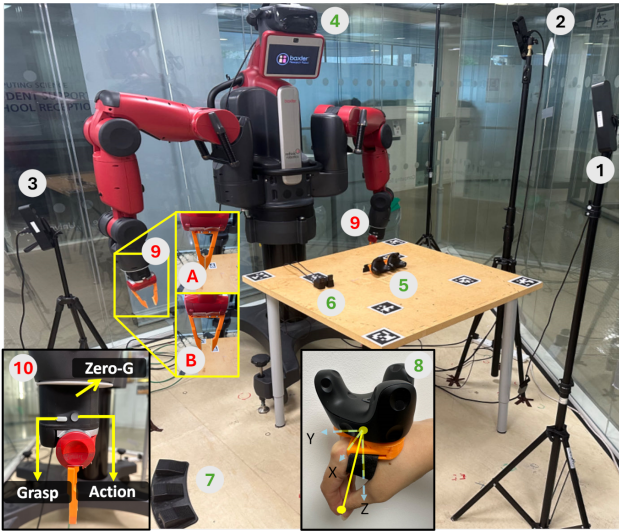


Fig. 2. Hardware Setup. (1) Front camera; (2) Top camera; (3) Side camera; (4) Steam Index VR Headset [20], which serves as the origin of the world; (5) HTC Vive tracker; (6) Receiver of the tracker; (7) Pedal; (8) Grasping Point, the yellow line indicates the distance from the center of the tracker to the grasping point; (9) Baxter’s gripper with (A) the gripper in its closed state and (B) opened state; (10) Baxter’s zero-G mode [21] and control buttons. The black numbers mean that this hardware was used for human and robot demonstrations; red numbers, it was used in the robot demonstration dataset only, and green numbers, it was used only for human demonstration.

The setup for the robot dataset closely mirrored that for the human demonstrations. We used a Rethink Robotics Baxter robot equipped with custom 3D printed grippers¹ for improved grip (Fig. 2). To ensure consistency across both datasets, we again used three ZED2i cameras with the same camera positions as in the human demonstrations. Control of the robot arm presented unique challenges due to the complexity and duration of garment manipulation tasks. To optimize the operator’s speed, ease, maneuverability, control and the fidelity of the robot arm’s movements to human actions, we explored direct teleoperation [23] and immersive Virtual Reality (VR) teleoperation [24]. With the VR, the operator struggled with boundary detection of the garment due to resolution limitations. Teleoperation [23] was problematic as synchronous movement between the human hand and robotic arm obstructed the operator’s side view of the garment while repositioning the operator in front of the robot was impractical due to human joint movement limitations and the need to mirror the robot’s actions. To resolve these issues, we opted to directly manipulate Baxter’s arms in its zero-G mode [21], (Fig. 2), which allows the operator to move the arms without resistance from the motors, as well as to activate the gripper. This mode was activated by grasping the cuff over its groove. The operator used a ‘grasp’ button alongside an ‘action’ button to control the opening and closing of the gripper; gripper opening and closing states are shown in Fig. 2-A and B.

¹The STL files for the gripper used can be found at <https://cvas-ug.github.io/flat-n-fold>

B. ZED2i Camera Calibration

We place calibration boards at various positions on the table (see Figs. 2 and 1) for camera calibration and use OpenCV’s PnP solver [25] to estimate the relative camera pose with respect to the table. To establish the calibration board’s position relative to the headset, a tracker was positioned in the right corner of each board (designated as the origin in OpenCV). The collected data was averaged over 10 repetitions to robustly estimate the relative positions of each camera to the headset, ensuring accurate spatial data in our experiments.

C. Methodology

For the human demonstration dataset, we invited 20 participants to capture how they manipulate garments from crumpled to folded states. Participants, equipped with trackers on both hands, were asked to stand behind a table were briefed on movement guidelines before data collection commenced. These guidelines included avoiding finger bending and only performing pick-and-place actions, minimizing arm crossing, and gently shaking the garment for easier handling. They were also advised to keep their hands within the bounds of the table as much as possible. For robot demonstrations, an operator familiar with the robotic arm controlled the robot’s arms and grippers (Fig. 2-9).

The human and robot demonstration stages are illustrated in Fig. 1. For both, demonstrations began with the participants or robot operator grasping a crumpled garment from any point using either hand or gripper and lifting the garment from the table. The flattening stage was not standardized; hence, participants or robot operator grasped and manipulated the garment in the air until it was nearly flat and then laid on the table. After, they were allowed to make further adjustments to enhance the garment’s flatness. We split participants in terms of whether they followed a fixed folding strategy (i.e. *Fixed*) or their usual, natural way to fold garments in their daily life (i.e. *Daily-life*). We must note that 7 participants performed both strategies; hence, the *Fixed* strategy comprised 17 participants, while the *Daily-life* strategy comprised 10 participants. The participants carrying out the *Fixed* strategy adhered to a structured folding approach such that all participants had a similar folded garment at the end of the manipulation. This approach differs from the simpler folding methods used in previous studies and is intended to reflect realistic, practical folding techniques. The robot operator followed both strategies while folding garments.

1) *Data Format*: Both visual and action data were captured and stored using ROS2 bag files. We use nearest-timestep matching to synchronize images with action data (similar to [16]). This synchronization ensures that for each camera, the number of RGB images equals the number of depth images. Moreover, the quantity of synchronized action data matches the number of images, ensuring that camera data aligns with the corresponding action data.

In the human demonstration dataset, the action data comprises the position and rotation of the tracker’s center. For

TABLE II
STATISTICS OF OUR DATASET

Garment type	Human demonstration			Human-controlled robot		
	Fixed	Daily-life	Total	Fixed	Daily-life	Total
Napkin	91	138	229	76	40	116
Towel	36	55	91	40	20	60
LS-Shirt	55	80	135	80	38	118
SS-Shirt	66	99	165	80	37	117
Pant	56	80	136	79	40	119
Sweater	57	85	142	80	40	120
LS-Tshirt	61	91	152	78	40	118
SS-Tshirt	63	99	162	80	39	119
Total	485	727	1212	593	294	887

all participants, we measured the distance from the back of their hand to the tip of their index finger along the three axes (Fig. 2-8). These measurements were then used to calculate the position of the grasping point, ensuring that we captured the location where participants interacted with the garment. A fixed offset representing the gripper length is added for the robot dataset, allowing for consistent alignment across both datasets.

D. Dataset overview

Our human and robot demonstration datasets use 44 diverse garments from 8 categories: napkins, towels, pants, long-sleeved shirts (LS-shirt), short-sleeved shirts (SS-shirt), long-sleeved t-shirts (LS-tshirt), short-sleeved t-shirts (SS-tshirt), and sweaters. Each category includes five items, except for pants, which consist of six. The garments within each category vary in size and stiffness, covering a wide range of fabrics and material properties. The dataset consists of 1,212 individual flattening and folding sequences of human and 887 robot demonstrations. The data distribution across different categories and individual garments is shown in Tab. II.

1) *Human Demonstration Dataset*: Each sequence comprises RGB images and depth images from three cameras, action sequences (capturing both the position and rotation of trackers related to the headset), and the timing of finger interactions with the garment. Each sequence documents a complete process of flattening and folding the garment. Additionally, each sequence records the position and rotation at the gripping points and is annotated with multiple labels: clothing type, clothing name, and the folding strategy of the action (*Fixed* or *Daily-life*). As described in Sec. III-C, the *Fixed* strategy followed a standardized folding method, and the *Daily-life* strategy followed a natural, everyday folding technique.

2) *Robot Demonstration Dataset*: For the robot dataset, we collected 887 sequences using the same 44 garments as in the human demonstration dataset. This dataset comprises the robot’s joint states and the position and rotation at the center of the wrist reference frame relative to its world origin, in addition to the multi-view RGB images and depth images. We also recorded gripper opening and closing states.

IV. EXPERIMENTS

We first compare the diversity and complexity of Flat’n’Fold to existing datasets (Sec. IV-A). Then, we define two benchmarks for evaluating grasp prediction (Sec. IV-B) and sub-task decomposition (Sec. IV-C).

A. Quantifying the diversity of the dataset

We first measure the diversity and complexity of our dataset compared to RoboTurk [9], MIME [10], VideoFolding [2], and Semantic State Estimation [6], considering both action and visual information. As shown in Tab. III, we measure complexity and diversity for action information. For complexity, we calculate the variance of positions and rotations across different time intervals within each action sequence. Then, we take the mean across all videos to measure the dataset’s *average complexity*. To measure the *average diversity* of action sequences, we uniformly sampled each sequence for 300 time ticks across datasets. The variance across sequences at individual time points was then calculated and averaged over the sequence duration to determine the extent of variation among different action sequences.

For visual information (Tab. IV), we extract features from each video using a pre-trained I3D model [26] after standardizing to 256 frames across sequences for all datasets. We then calculate the global standard deviation of these features to measure diversity.

In Tables III and IV, a lower value means the dataset is less complex and diverse. For action diversity, both the human and robot demonstration datasets exhibit significantly higher position standard deviation than other datasets. Specifically, the position standard deviation for average complexity in human demonstrations (Tab. III) surpasses that of RoboTurk by 133.33% and MIME by 3219.51%. Similarly, the rotation standard deviation (Euler angle) for average complexity in human-controlled robot demonstrations exceeds that of RoboTurk by 14.63% and MIME by 38.56%. This trend can also be observed for visual diversity, where the standard deviation in our human demonstration dataset is 7.91% greater than that observed in VideoFolding for comparable tasks. Similarly, our human-controlled robot dataset’s standard deviation exceeds RoboTurk’s by 5.33%. We can, therefore, conclude that Flat’n’Fold shows a broader range of visual and action data and demonstrates the applicability of our dataset in diverse settings for garment perception and manipulation.

B. Grasping Point Prediction Benchmark

Grasping point prediction is an essential subtask for garment manipulation but remains challenging in part due to a lack of comprehensive training datasets with annotated ground truth. Research into garment grasping points has been confined mainly to simplistic scenarios, such as picking up centrally located points on crumpled fabrics, garments on a flat surface [27] or grasping garments hung on hangers [28]. Our dataset addresses this gap by providing annotated

TABLE III
COMPARATIVE ANALYSIS FOR ACTION DIVERSITY.

Dataset	Human				Robot			
	Average Complexity		Average Diversity		Average Complexity		Average Diversity	
	Position	Rotation	Position	Rotation	Position	Rotation	Position	Rotation
Roboturk [9]	-	-	-	-	0.105	14.907	0.123	16.564
MIME [10]	-	-	-	-	7.38×10^{-3}	12.335	7.21×10^{-3}	4.742
Flat'n'Fold (ours)	0.245	10.726	0.219	5.560	0.217	17.089	0.176	16.894

* Position is given in meters and rotation in radians

TABLE IV
COMPARATIVE ANALYSIS FOR VIDEO DIVERSITY

Dataset	Human	Robot
Roboturk [9]	-	589.99
MIME [10]	377.65	473.12
Videofolding [2]	688.07	-
Semantic state est. [6]	428.10	375.77
Ours	742.53	621.45

grasping points while manipulating garments from a crumpled state to a folded state.

To establish a benchmark for subsequent studies, we define a subset of our dataset comprising points in time when the hand/gripper is about to grasp the garment. We extract ground truth information at the instant of grasping, i.e. which hand grasps the garment (left/right), its position and its rotation. We extract point-clouds from 8 to 10 frames earlier, fusing the three views and segmenting to include only the garment; this avoids leakage of the arm position for grasping prediction. This yields 6,329 annotated point clouds from the human subset and 5,574 from the robot subset. The goal is then to predict the optimal grasp location given a point-cloud. As metrics, we measure the classification accuracy (left vs right hand), the L1 error of positions and the geodesic error of rotations. The dataset is divided into training, validation, and testing sets in a 7:1:2 ratio across all garment types.

As baselines, we evaluate two popular models operating on point-clouds, PointNet++ [29] and Point-BERT [30]. Both were pretrained on ModelNet-40, and we added two fully-connected layers to predict hand position (supervised with an L1 loss), rotation quaternion (with geodesic loss), and left/right hand (with cross-entropy loss). We conducted two experiments using these models to examine the effects of varying dataset sizes and garment types on the outcomes.

In Tab. V, we show results when training on different fractions of our dataset. All metrics consistently improve with the amount of training data in human and robot demonstrations, which shows the value of using a large-scale dataset for grasping garments. For example, on the human demonstrations subset, PointNet++'s classification accuracy increases from 55.7% using 20% of training data to 59.9% with the full training set, with corresponding reductions in position error (from 0.103 meters to 0.1 meters) and rotation error (from 0.028 radians to 0.023 radians). However, even with the full dataset, the results are still far from perfect which indicates

TABLE V
GRASPING POINT PREDICTION WITH POINTNET++ AND POINT-BERT

Model	Dataset Size	Classification acc.		Position error		Rotation error	
		Human	Robot	Human	Robot	Human	Robot
PointNet++ [29]	20%	0.557	0.669	0.103	0.092	0.028	0.048
	50%	0.586	0.707	0.102	0.084	0.025	0.047
	100%	0.599	0.710	0.100	0.076	0.023	0.043
Point-BERT [30]	20%	0.606	0.658	0.101	0.073	0.023	0.049
	50%	0.620	0.683	0.103	0.072	0.022	0.048
	100%	0.625	0.747	0.096	0.067	0.022	0.045

* Position error is given in meters and rotation error in radians

TABLE VI
PERFORMANCE COMPARISON OF POINTNET++ AND POINT-BERT

	PointNet++						Point-BERT					
	Class. Acc.		Pos. Error		Rot. Error		Class. Acc.		Pos. Error		Rot. Error	
	H	R	H	R	H	R	H	R	H	R	H	R
Napkin	0.590	0.850	0.085	0.078	0.036	0.048	0.532	0.897	0.065	0.071	0.039	0.040
Towel	0.606	0.647	0.091	0.102	0.027	0.074	0.634	0.686	0.093	0.083	0.028	0.076
SS-shirt	0.661	0.747	0.118	0.070	0.019	0.050	0.719	0.635	0.093	0.061	0.016	0.060
SS-tshirt	0.657	0.671	0.121	0.067	0.023	0.053	0.729	0.671	0.108	0.053	0.021	0.061
LS-shirt	0.549	0.667	0.102	0.083	0.023	0.056	0.576	0.648	0.086	0.069	0.021	0.052
LS-tshirt	0.633	0.630	0.093	0.076	0.024	0.042	0.622	0.674	0.080	0.081	0.025	0.065
Sweater	0.606	0.746	0.091	0.078	0.027	0.028	0.592	0.651	0.076	0.071	0.023	0.042
Pant	0.558	0.776	0.101	0.070	0.035	0.052	0.475	0.834	0.087	0.065	0.038	0.039
Average	0.607	0.717	0.1	0.078	0.027	0.05	0.61	0.712	0.086	0.069	0.026	0.054

* Position error is given in meters and rotation error in radians

that existing methods struggle to predict grasps accurately and that future research has significant room for improvement. By comparing the two subsets, robot demonstrations outperform human demonstrations with higher classification accuracy and lower position errors across both methods but with higher rotation errors. The difference lies in the fact that robot demonstrations have a wider range of variation in the rotation component compared to human demonstrations (see Tab. III), causing the baseline models to generate higher rotation errors. Notably, for position errors, where robot demonstrations show less diversity, the errors are smaller.

In Tab. VI, we show results split by garment type. In the table, *Class. Acc.* is Classification Accuracy, *Pos. Error* is Position Error, and *Rot. Error* is the Rotation Error. *H* represents Human demonstrations and 'R' Robot demonstrations. For human demonstrations, we can observe that shirts (SS-shirt and SS-tshirt) have higher classification accuracy and lower rotation errors but higher position errors. In contrast, napkins have higher position errors but higher rotation errors. Pants, on the other hand, show lower classification accuracy. In robot demonstrations, towels have both higher position and rotation errors. These results indicate that these four garment types should be a particular focus for future work.

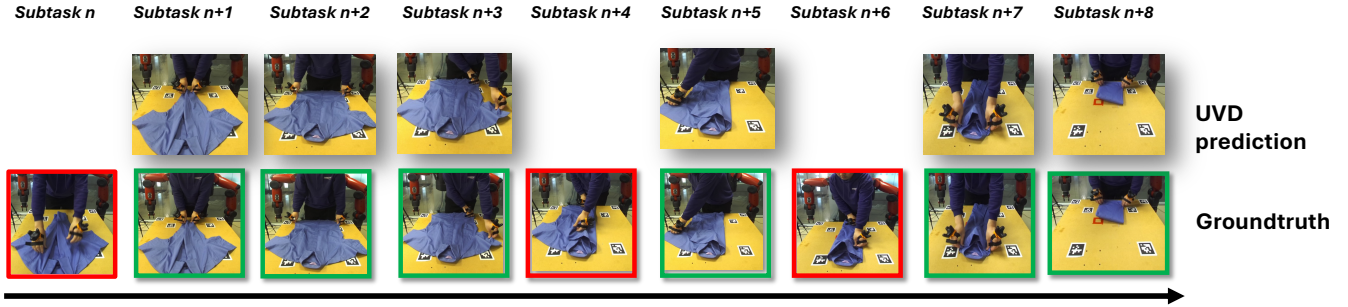


Fig. 3. Example of subtask decomposition with Flat’n’Fold using UVD [31] alongside ground truth comparisons. Green blocks represent accurately predicted subtasks by UVD, while red blocks indicate ground truth subtask images that UVD failed to identify.

TABLE VII

QUANTITATIVE RESULTS FOR UVD COMPARED ACROSS HUMAN AND ROBOT DATASETS AND FLATTENING/FOLDING PHASES

		Precision	Recall	F1
Human	Flattening	0.520	0.658	0.564
	Folding	0.905	0.582	0.695
	Total	0.713	0.620	0.629
Robot	Flattening	0.416	0.331	0.356
	Folding	0.825	0.391	0.523
	Total	0.621	0.361	0.441

TABLE VIII

QUANTITATIVE RESULTS FOR UVD [31] ON HUMAN VIDEOS OF DIFFERENT FOLDING STRATEGIES

Strategy	Precision	Recall	F1
Fixed	0.905	0.582	0.695
Daily-life	0.894	0.571	0.684

C. Automated Subtask Decomposition Benchmark

Mastering long-horizon manipulation tasks such as flattening and folding remains challenging. One approach is to break them into smaller, more manageable subtasks to effectively learn these tasks and generalize to new situations. We, therefore, use our dataset to define a benchmark for task decomposition methods; an example of task decomposition can be found in Fig. 3.

We define ‘*pick*’ and ‘*place*’ actions ground-truth sub-task boundaries. Specifically, we divide each image sequence into two phases. During the *flattening* phase, we treat every pick action as a subtask but not place since these often cause no change to the garment. During the *folding* phase, we treat every pick or place as a subtask. During the evaluation, we consider a predicted subtask boundary correct if it is within 10 frames of the annotated ground truth; based on this, we calculate the precision, recall, and F1 score.

As a baseline, we evaluate the state-of-the-art unsupervised task decomposition UVD [31], using VIP [32] as the visual encoder. Results are shown in Tab. VII. The precision for both human demonstration and robot demonstration is relatively high at 0.713 and 0.621, respectively. This shows that the method accurately identifies relevant subtasks when

the actions involve direct manipulation on a stable surface. However, lower recall rates of 0.620 for humans and 0.361 indicate that many subtask boundaries are missed. For both subsets, precision varied across phases, with a lower rate of 0.520 and 0.416 during flattening but a much higher rate of 0.905 and 0.825 during folding. When comparing the two subsets, the UVD method demonstrates better performance across all metrics in human demonstrations.

We also further analyzed whether different folding strategies affect the effectiveness of UVD. The results from Tab. VIII show that varied folding approaches introduce complexities that affect the UVD method’s performance. Specifically, participants folding garments in their style (Daily-life) demonstrated lower precision (0.894) and recall (0.571) compared to those following predefined rules (Fixed), which achieved a precision of 0.905 and a recall of 0.582, resulting in an F1 score of 0.684. The latter indicates that there is a need to develop approaches that can capture more diverse manipulation strategies.

V. CONCLUSION

We have introduced Flat’n’Fold, a dataset comprising over 1,212 human and 887 robot demonstrations of flattening and folding 44 unique garments spanning eight categories. Flat’n’Fold contains high-resolution multi-view RGB-D and point cloud data, as well as ground-truth actions. We have also defined two new benchmarks for garment manipulation tasks: grasping point prediction and subtask decomposition. In the future, the size and scope of our dataset can enable training and benchmarking on new tasks. By providing diverse human actions, the dataset can be used for imitation learning, enabling robots to learn complex manipulation tasks. Additionally, Flat’n’Fold’s multimodality can support the future development of models that accurately perceive and predict the state of garments, which is essential for improving the performance of cloth pose estimation and planning manipulation tasks.

ACKNOWLEDGMENT

We want to thank Zhuo He, Tanatta Chaichakan, and the Computer Vision and Autonomous Systems (CVAS) research group for insightful discussions and for participating in the data collection for this work.

REFERENCES

- [1] L. Sun, G. Aragon-Camarasa, S. Rogers, and J. P. Siebert, "Accurate garment surface analysis using an active stereo robot head with application to dual-arm flattening," in *2015 IEEE international conference on robotics and automation (ICRA)*. IEEE, 2015, pp. 185–192.
- [2] A. Verleysen, M. Biondina, and F. Wyffels, "Video dataset of human demonstrations of folding clothing for robotic folding," *Int. J. Robotics Res.*, vol. 39, no. 9, 2020. [Online]. Available: <https://doi.org/10.1177/0278364920940408>
- [3] L. Duan and G. Aragon-Camarasa, "A continuous robot vision approach for predicting shapes and visually perceived weights of garments," *IEEE Robotics and Automation Letters*, vol. 7, no. 3, pp. 7950–7957, 2022.
- [4] Y. Avigal, L. Berscheid, T. Asfour, T. Kröger, and K. Goldberg, "Speedfolding: Learning efficient bimanual folding of garments," in *2022 IEEE/RSJ International Conference on Intelligent Robots and Systems (IROS)*, 2022, pp. 1–8.
- [5] A. Bozic, M. Zollhöfer, C. Theobalt, and M. Nießner, "Deepdeform: Learning non-rigid RGB-D reconstruction with semi-supervised data," in *2020 IEEE/CVF Conference on Computer Vision and Pattern Recognition, CVPR 2020, Seattle, WA, USA, June 13-19, 2020*. Computer Vision Foundation / IEEE, 2020, pp. 7000–7010. [Online]. Available: https://openaccess.thecvf.com/content_CVPR_2020/html/Bozic_DeepDeform_Learning_Non-Rigid_RGB-D_Reconstruction_With_Semi-Supervised_Data_CVPR_2020_paper.html
- [6] G. Tzelepis, E. E. Aksoy, J. B. Sol, and G. Alenyà, "Semantic state estimation in cloth manipulation tasks," *CoRR*, vol. abs/2203.11647, 2022. [Online]. Available: <https://doi.org/10.48550/arXiv.2203.11647>
- [7] H. Xue, W. Xu, J. Zhang, T. Tang, Y. Li, W. Du, R. Ye, and C. Lu, "Garmenttracking: Category-level garment pose tracking," in *IEEE/CVF Conference on Computer Vision and Pattern Recognition, CVPR 2023, Vancouver, BC, Canada, June 17-24, 2023*. IEEE, 2023, pp. 21 233–21 242. [Online]. Available: <https://doi.org/10.1109/CVPR52729.2023.02034>
- [8] A. Boix-Granell, S. Foix, and C. Torras, "Garment manipulation dataset for robot learning by demonstration through a virtual reality framework," in *Artificial Intelligence Research and Development - Proceedings of the 24th International Conference of the Catalan Association for Artificial Intelligence, CCIA 2022, Stiges, Spain, 19-21 October 2022*, ser. Frontiers in Artificial Intelligence and Applications, A. Cortés, G. Grimaldo, and T. Flaminio, Eds., vol. 356. IOS Press, 2022, pp. 199–208. [Online]. Available: <https://doi.org/10.3233/FAIA220338>
- [9] A. Mandlekar, J. Booher, M. Spero, A. Tung, A. Gupta, Y. Zhu, A. Garg, S. Savarese, and L. Fei-Fei, "Scaling robot supervision to hundreds of hours with roboturk: Robotic manipulation dataset through human reasoning and dexterity," in *2019 IEEE/RSJ International Conference on Intelligent Robots and Systems, IROS 2019, Macau, SAR, China, November 3-8, 2019*. IEEE, 2019, pp. 1048–1055. [Online]. Available: <https://doi.org/10.1109/IROS40897.2019.8968114>
- [10] P. Sharma, L. Mohan, L. Pinto, and A. Gupta, "Multiple interactions made easy (MIME): large scale demonstrations data for imitation," in *2nd Annual Conference on Robot Learning, CoRL 2018, Zürich, Switzerland, 29-31 October 2018, Proceedings*, ser. Proceedings of Machine Learning Research, vol. 87. PMLR, 2018, pp. 906–915. [Online]. Available: <http://proceedings.mlr.press/v87/sharma18a.html>
- [11] C. Wang, L. Fan, J. Sun, R. Zhang, L. Fei-Fei, D. Xu, Y. Zhu, and A. Anandkumar, "Mimicplay: Long-horizon imitation learning by watching human play," in *Conference on Robot Learning, CoRL 2023, 6-9 November 2023, Atlanta, GA, USA*, ser. Proceedings of Machine Learning Research, J. Tan, M. Toussaint, and K. Darvish, Eds., vol. 229. PMLR, 2023, pp. 201–221. [Online]. Available: <https://proceedings.mlr.press/v229/wang23a.html>
- [12] A. Mandlekar, D. Xu, J. Wong, S. Nasiriany, C. Wang, R. Kulkarni, L. Fei-Fei, S. Savarese, Y. Zhu, and R. Martín-Martín, "What matters in learning from offline human demonstrations for robot manipulation," in *arXiv preprint arXiv:2108.03298*, 2021.
- [13] E. Johns, "Coarse-to-fine imitation learning: Robot manipulation from a single demonstration," in *IEEE International Conference on Robotics and Automation (ICRA)*, 2021.
- [14] L. Duan and G. Aragon-Camarasa, "A data-centric approach for dual-arm robotic garment flattening," *arXiv preprint arXiv:2208.13695*, 2022.
- [15] M. Moletta, M. K. Wozniak, M. C. Welle, and D. Kragic, "A virtual reality framework for human-robot collaboration in cloth folding," in *22nd IEEE-RAS International Conference on Humanoid Robots, Humanoids 2023, Austin, TX, USA, December 12-14, 2023*. IEEE, 2023, pp. 1–7. [Online]. Available: <https://doi.org/10.1109/Humanoids57100.2023.10375184>
- [16] C. Chi, Z. Xu, C. Pan, E. Cousineau, B. Burchfiel, S. Feng, R. Tedrake, and S. Song, "Universal manipulation interface: In-the-wild robot teaching without in-the-wild robots," in *Proceedings of Robotics: Science and Systems (RSS)*, 2024.
- [17] C. Chi, S. Feng, Y. Du, Z. Xu, E. Cousineau, B. Burchfiel, and S. Song, "Diffusion policy: Visuomotor policy learning via action diffusion," *CoRR*, vol. abs/2303.04137, 2023. [Online]. Available: <https://doi.org/10.48550/arXiv.2303.04137>
- [18] Y. Ze, G. Zhang, K. Zhang, C. Hu, M. Wang, and H. Xu, "3d diffusion policy: Generalizable visuomotor policy learning via simple 3d representations," in *ICRA 2024 Workshop on 3D Visual Representations for Robot Manipulation*, 2024.
- [19] Z. Liu, P. Luo, S. Qiu, X. Wang, and X. Tang, "Deepfashion: Powering robust clothes recognition and retrieval with rich annotations," in *2016 IEEE Conference on Computer Vision and Pattern Recognition, CVPR 2016, Las Vegas, NV, USA, June 27-30, 2016*. IEEE Computer Society, 2016, pp. 1096–1104. [Online]. Available: <https://doi.org/10.1109/CVPR.2016.124>
- [20] Valve Corporation, "Valve index," <https://store.steampowered.com/valveindex>, 2019, accessed: 2019-12-31.
- [21] Rethink Robotics, "Arm control system," <https://support.rethinkrobotics.com/support/solutions/articles/80000980284-arm-control-system>, 2022, accessed: 2024-08-05.
- [22] store.steampowered.com, "Steamvr on steam," <https://store.steampowered.com/app/250820/SteamVR/>, 2024, accessed: 2024-08-05.
- [23] F. P. Audonnet, J. Grizou, A. Hamilton, and G. Aragon-Camarasa, "Telesim: A modular and plug-and-play framework for robotic arm teleoperation using a digital twin," in *2024 IEEE International Conference on Robotics and Automation (ICRA)*. IEEE, 2024, pp. 17 770–17 777.
- [24] F. Audonnet, I. Ramirez-Alpizar, and G. Aragon-Camarasa, "Immer-twin: A mixed reality framework for enhanced robotic arm teleoperation," under review in *ICRA2025*, 2024.
- [25] M. A. Fischler and R. C. Bolles, "Random sample consensus: A paradigm for model fitting with applications to image analysis and automated cartography," *Commun. ACM*, vol. 24, no. 6, pp. 381–395, 1981. [Online]. Available: <https://doi.org/10.1145/358669.358692>
- [26] P. Gupta, A. Thatipelli, A. Aggarwal, S. Maheshwari, N. Trivedi, S. Das, and R. K. Sarvadevabhatla, "Quo vadis, skeleton action recognition?" *Int. J. Comput. Vis.*, vol. 129, no. 7, pp. 2097–2112, 2021. [Online]. Available: <https://doi.org/10.1007/s11263-021-01470-y>
- [27] H. Shehawy, P. Rocco, and A. M. Zanchettin, "Estimating a garment grasping point for robot," in *20th International Conference on Advanced Robotics, ICAR 2021, Ljubljana, Slovenia, December 6-10, 2021*. IEEE, 2021, pp. 707–714. [Online]. Available: <https://doi.org/10.1109/ICAR53236.2021.9659444>
- [28] F. Zhang and Y. Demiris, "Learning grasping points for garment manipulation in robot-assisted dressing," in *2020 IEEE International Conference on Robotics and Automation, ICRA 2020, Paris, France, May 31 - August 31, 2020*. IEEE, 2020, pp. 9114–9120. [Online]. Available: <https://doi.org/10.1109/ICRA40945.2020.9196994>
- [29] C. R. Qi, L. Yi, H. Su, and L. J. Guibas, "Pointnet++: Deep hierarchical feature learning on point sets in a metric space," in *Advances in Neural Information Processing Systems 30: Annual Conference on Neural Information Processing Systems 2017, December 4-9, 2017, Long Beach, CA, USA*, I. Guyon, U. von Luxburg, S. Bengio, H. M. Wallach, R. Fergus, S. V. N. Vishwanathan, and R. Garnett, Eds., 2017, pp. 5099–5108. [Online]. Available: <https://proceedings.neurips.cc/paper/2017/hash/d8bf84be3800d12f74d8b05e9b89836f-Abstract.html>
- [30] X. Yu, L. Tang, Y. Rao, T. Huang, J. Zhou, and J. Lu, "Point-bert: Pre-training 3d point cloud transformers with masked point modeling," in *IEEE/CVF Conference on Computer Vision and Pattern Recognition, CVPR 2022, New Orleans, LA, USA, June 18-24, 2022*. IEEE, 2022, pp. 19 291–19 300. [Online]. Available: <https://doi.org/10.1109/CVPR52688.2022.01871>
- [31] Z. Zhang, Y. Li, O. Bastani, A. Gupta, D. Jayaraman, Y. J. Ma, and

- L. Weihs, “Universal visual decomposer: Long-horizon manipulation made easy,” in *2024 IEEE International Conference on Robotics and Automation (ICRA)*. IEEE, 2024, pp. 6973–6980.
- [32] Y. J. Ma, S. Sodhani, D. Jayaraman, O. Bastani, V. Kumar, and A. Zhang, “Vip: Towards universal visual reward and representation via value-implicit pre-training,” *arXiv preprint arXiv:2210.00030*, 2022.